

EHD flow produced by positive and negative point-to-plate corona discharges

Eric Moreau, Patrick Braud, Etienne Defoort, Nicolas Benard
University of Poitiers,
Institut Pprime, CNRS-ISAE-ENSMA, France
e-mail: eric.moreau@univ-poitiers.fr

Abstract—In this study, we aim at characterizing the ionic wind EHD flow produced by corona discharges ignited between a high voltage needle and a grounded plate electrode. First, the morphology of these discharges is observed using an iCCD camera and compared to current measurements. Secondly, the ionic wind produced by these different discharges is characterized by time-resolved particle image velocimetry (PIV) measurements. For that, quiescent air is seeded with dielectric oil droplets and images are acquired using a high-speed camera set to 20kHz. These measurements allow us to characterize precisely the ionic wind versus time, as well as its dynamics when the discharge is switched on. In all the cases, we observe that at the discharge ignition, a jet starts from the needle and then it moves toward the plate, resulting in a wall-impinging jet with a vortex ring. When the jet is well-established, the ionic wind evolution versus time depends strongly on the high voltage polarity. Indeed, a negative DC corona discharge produces a steady ionic wind with weak velocity fluctuations. On the contrary, the positive corona discharge induces a faster ionic wind, showing that it is more efficient than the negative one, more especially when the breakdown streamer regime appears. In this case, the mean velocity is nearly constant in the region located between the point and the plate, meaning that there is still a EHD force in the inter-electrode gap, which is able to counter the viscous effects. Furthermore, we observe that, in presence of streamers, the corona discharge produces a pulsed ionic wind whose frequency corresponds to the frequency of the streamer occurrence. Finally, we demonstrate that each discharge current pulse corresponds to one primary streamer followed by several secondary streamers. Then, just after the development of these secondary streamers, a significant positive space charge remains in the inter-electrode gap, resulting in a high EHD force.

I. INTRODUCTION

When a high potential difference is applied between two electrodes in atmospheric air, ionization of the air molecules around the thinnest electrode induces a corona discharge. Due to the electric field, the produced ions are submitted to Coulomb force, resulting in their motion from the active electrode toward the grounded collecting one. The set of all these Coulomb forces results in a volume electrohydrodynamic (EHD) force occurring inside the discharge. Hence, in the electrode gap, many collisions between ions in motion and neutral air molecules take place, resulting in a momentum transfer that produces a gas flow, which is usually called “ionic wind”.

In the present paper, we focus on the electrohydrodynamic phenomena occurring inside corona discharges in atmospheric air. We propose to detail the ionic wind produced when the discharge is ignited and to compare negative and positive coronas. For that pur-

pose, we have developed a multi-metrology experimental bench including electrical measurements, iCCD visualizations and time-resolved particle image velocimetry.

II. EXPERIMENTAL SETUP

To produce the discharge, a high voltage (HV) is applied between a needle and a grounded plane electrode. Both electrodes are made of stainless-steel and are separated by a gap of 25 mm (Fig. 1). The needle electrode has a tip having a curvature radius equal to about 100 μm . The plane electrode has a disk shape with rounded edges and a diameter of 80 mm. The high voltage is generated by a HV amplifier (Trek 30kV/40mA) and it is measured with a probe (North StarPVM-1, 500 MHz). The discharge current waveform is visualized with a second probe (Lecroy, PP018, 500 MHz, 10 pF) that measures the voltage across a 1 k Ω resistor set between the plate and earth. All the signals can be simultaneously recorded with a digital oscilloscope (Lecroy HDO6054, 500 MHz, 2.5 GS $\cdot\text{s}^{-1}$).

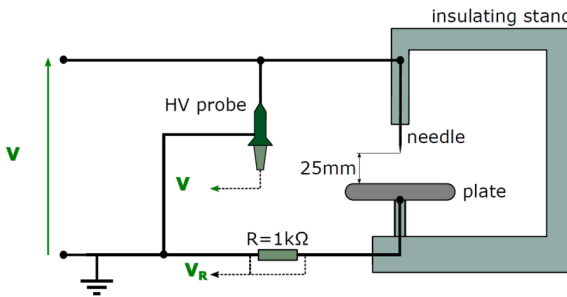


Fig. 1. Setup of the corona discharge.

Images of the discharge are recorded by a fast gateable iCCD camera (Princeton, Pi-max4 Gen2) with a resolution of 1024 \times 1024 pixels² and equipped with a 60 mm objective. The final field of view corresponds to a 39 \times 39 mm² region (38 μm per pixel).

To characterize the ionic wind produced by the discharge, a LaVision time-resolved particle imaging velocimetry (PIV) system is used. The point-to-plane design presented in Fig. 1 is put into a PMMA tank (30 \times 80 \times 40 cm³). The air is seeded with dielectric oil droplets (Ondina 915) having a mean diameter equal to 0.3 μm . It has been demonstrated that these particles did not submit electrostatic precipitation, meaning that they followed well the produced airflow without sleeping. A 532 nm Nd:YAG laser generator (Continuum Mesa), equipped with a divergent cylindrical lens, is used to provide a laser sheet that illuminates the particles in the x-y plane, passing through the tip of the needle and the middle of the plate ($z = 0$). Images are acquired using a high-speed camera (Photron Fastcam SA-Z), with a resolution of 1024 \times 1024 pixels² and equipped with a 60 mm lens. The resulting images have a size of 30 \times 30 mm². The acquisition frequency is set to 20 kHz, leading to a time delay of 50 μs between two consecutive images. In total, 3000 images are acquired for each experiment. The vector fields are computed using a cross-correlation algorithm with adaptive multi-passes, interrogation windows of 64 \times 64 down to 16 \times 16 pixels² and an overlap set to 50%, leading to a final flow field resolution of one vector every 266 μm .

III. RESULTS

A. Electrical and Optical Measurements

Fig. 2 presents the evolution of the time-averaged discharge current versus applied high voltage, in the case of positive and negative coronas (I-V characteristics). Several remarks can be formulated. First, as expected, we can see that the negative discharge results in a higher current than the positive one. Secondly, even if this kind of discharge involves complex phenomena, a simple empirical expression, called Townsend's equation [1], can be generally used to link the evolution of the current discharge as a function of the applied voltage V :

$$I = C \times V (V - V_0) \quad (1)$$

where V is the applied DC voltage, V_0 the discharge onset voltage and C a constant depending on the voltage polarity, electrode configuration, temperature, pressure and gas composition. As we can see in Fig. 2, this equation allows us to interpolate correctly the experimental measures in the case of the negative corona. On the contrary, for the positive corona, the discharge current follows well Eq. (1) when V is equal or smaller than 14 kV, but when V becomes higher than 14 kV, the current starts to evolve linearly with the voltage. By the past, several authors have already reported some difference between the Townsend's equation and experimental measurements, these differences being observed generally at low current values and depending on the electrode geometry or relative air humidity [2]. However, to our knowledge, it is the first time that this kind of behavior is clearly reported. Hence, in order to identify the reasons why the positive current suddenly increased when V reached 14 kV, we decided to visualize the discharge with a iCCD camera and to record the discharge current versus time for both positive and negative coronas (Fig. 3 and 4). These measurements should allow us to characterize the different discharge regimes.

In the case of a positive corona, for voltages smaller than +14 kV, we observe the stable Hermstein's glow regime characterized by a small ionized region concentrated around the tip of the high voltage electrode (see the case $V = +12$ kV in Fig. 3). The discharge current is then constant, and equal to a few μA (not visible in Fig. 3 because the current scale is in mA). Over +14 kV, we can see some luminous ionized channels that cross the electrode gap. Close to the threshold value of +14 kV, only a few pulses are erratically present in the discharge current, but as the applied voltage increases, the amplitude and the repetition rate of the current pulses increase and the time interval between two consecutive current peaks becomes more uniform, around a few kilohertz. For $V > +14$ kV, the breakdown streamer regime is established, the transition between both regimes occurring around +14 kV. Hence, if we return to Fig. 2, we can assume that Eq. (1) fits correctly the measured current when the discharge is glow. However, when the breakdown streamer appears, the pulsed component of the current which is added to the DC one, results in a shift of the total current compared to the Townsend's equation.

In the case of a negative corona, when the discharge ignites, we have been able to observe some current peaks for voltage down to -6 kV (not shown here); this is the Trichel pulse regime. Then, when the voltage magnitude is increased (*i.e.* $V < -6$ kV), the current is fully constant with time; this is the pulseless corona regime. Looking at the iCCD visu-

alizations (Fig. 4), we can see that the light emitted by the negative discharge is concentrated around the tip of the active electrode, without any negative streamers.

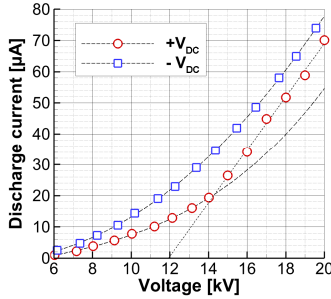


Fig. 2. Time-averaged discharge current versus applied voltage V_{DC} (negative corona : blue squares, positive corona : red circles).

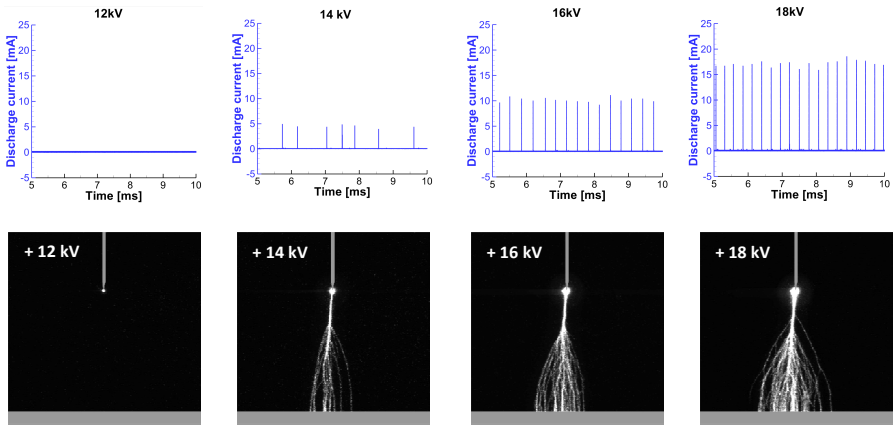


Fig. 3. Discharge current versus time and corresponding iCCD snapshots for a positive corona discharge, for voltages from +12 kV to +18 kV. For the iCCD acquisitions, the camera shutter is opened during 2 ms. The electrodes appear in grey, with an electrode gap of 25 mm.

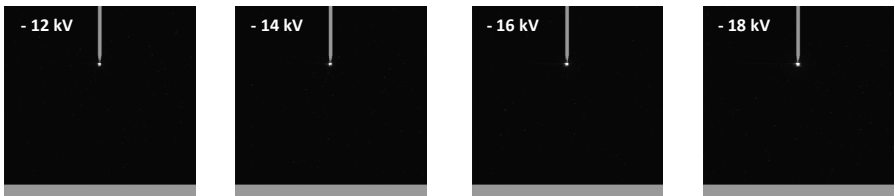


Fig. 4. iCCD snapshots of a negative discharge, for voltages from -12 kV to -18 kV. The camera shutter is opened during 2 ms. The electrodes appear in grey, with an electrode gap of 25 mm.

B. Velocity Measurements

After characterizing electrical and optical properties of both positive and negative coronas, we focus now on the discharge hydrodynamics, that is to say the produced ionic wind. First, we aim at characterizing the time-resolved EHD flow when the discharge is switched on.

Fig. 5 presents the instantaneous velocity vector fields at different times ($t = 1, 2, 4, 8$ and 12 ms, the high voltage being switched on at $t = 0$) for $+16$ kV and -16 kV. The needle is located at $x = 0$ and $y = 0$ when the plane electrode is located at $x = 25$ mm. In the case of a positive corona, a thin jet starts from the needle with a velocity higher than 5 m/s, 1 ms after the discharge ignition. Then the jet progresses rapidly toward the plane and reaches it in a few milliseconds, resulting in a wall-impinging jet with two vortices that rotates in opposite directions. This underlines that a three-dimensional axisymmetric annular vortex is developing against the wall. The results obtained with the negative corona show that the ionic wind jet is wider and slower.

Fig. 6 presents the time-averaged velocity fields for positive and negative corona discharges, for different voltage values. First, one can see that the topology of the flow produced by a positive discharge is fully different compared to the one of a negative discharge. For the negative corona, the maximum velocity is concentrated in a region close to the tip and this region grows and spreads progressively toward the plate when the high voltage is increased. More, the velocity decreases along the vertical axis X, meaning that the EHD force occurs only very close to the tip (even at -16 kV), inside the ionization region. Then, when one moves away from the tip, the ionic wind velocity decreases because of the viscous effects. For the positive corona discharge, the voltage effect is fully different. Up to $+12$ kV, the region of maximum velocity is located near the needle. However, from $+14$ kV, when the breakdown streamer regime appears, the mean velocity becomes constant along the x axis, meaning that there is still a weak EHD force in the inter-electrode gap. This force, which is able of countering the viscous forces, highlights that the presence of streamers results in a significant remaining positive space charge in the whole inter-electrode gap.

Finally, Fig. 7 shows that the appearance of streamers results in an unsteady flow. Indeed, for negative coronas (at -12 kV and -16 kV), the RMS values of the velocity is limited to a few percents of the time-averaged velocity. For positive coronas, it is also the case at $+12$ kV. However, at $+16$ kV, the RMS values reaches 0.1 in the electrode gap, where the discharge occurs. This means that the ionic wind flow is steady when the current is constant and that there are strong velocity fluctuations, resulting in an unsteady ionic wind jet when the discharge regime is the breakdown streamer one.

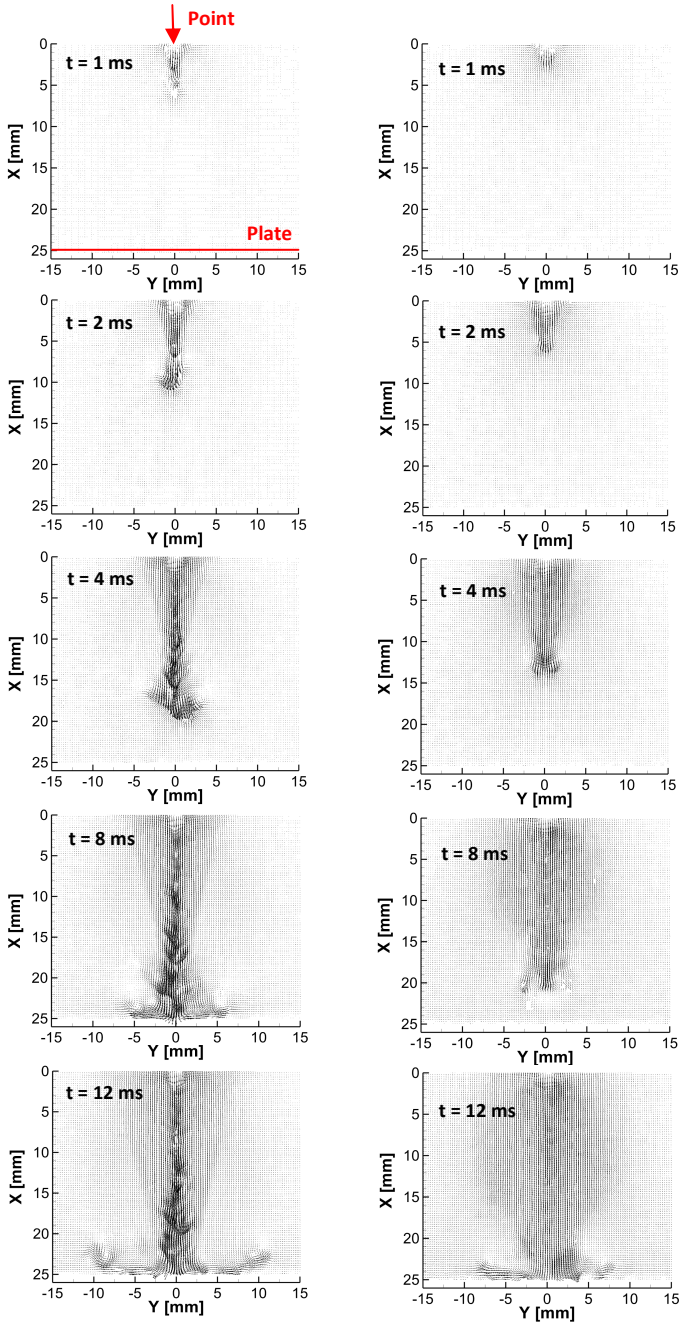


Fig. 5. Instantaneous velocity vector fields at $t = 1, 2, 4, 8$ and 12 ms for positive (on left) and negative (on right) corona discharges. The high voltage of ± 16 kV is switched on at $t = 0$.

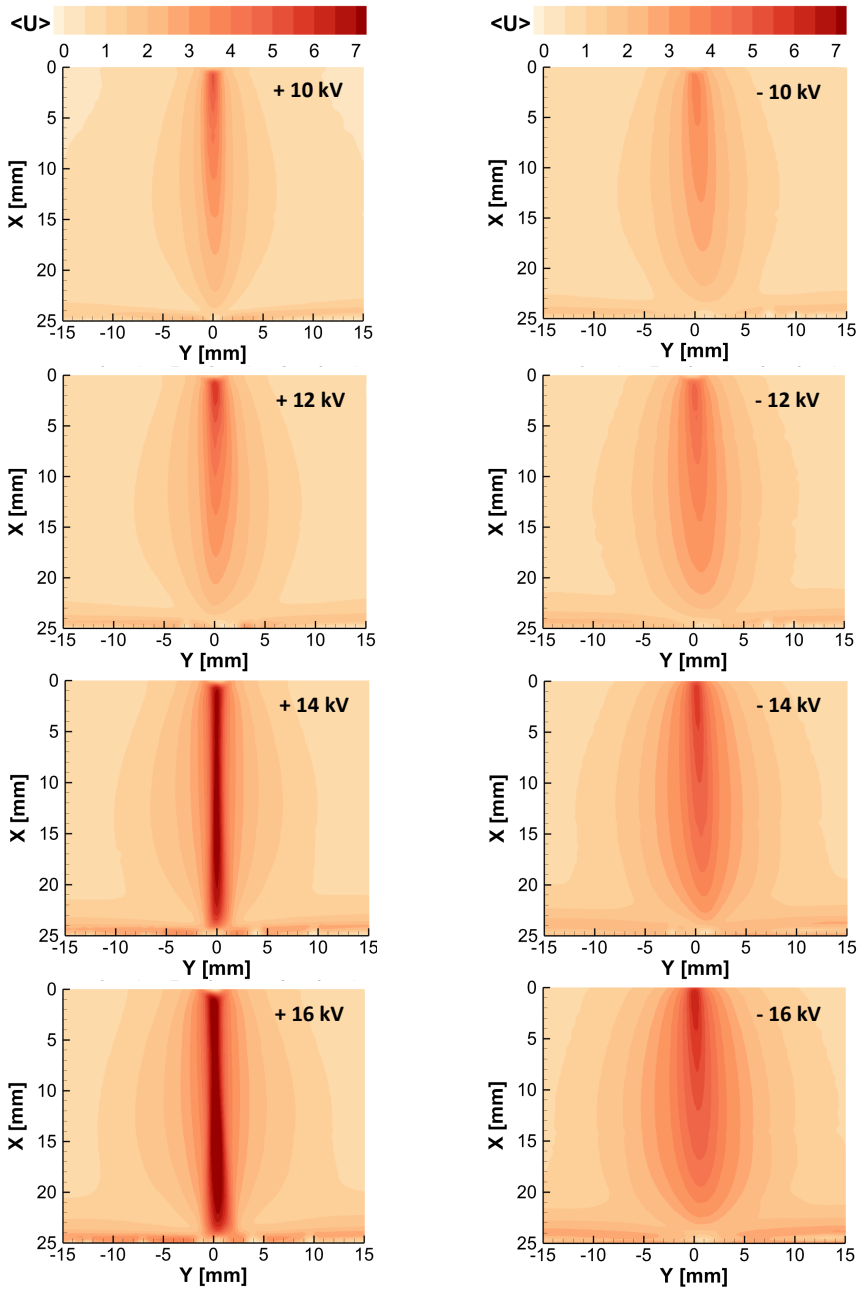


Fig. 6. time-averaged velocity fields for positive and negative corona discharges, for different voltage values.

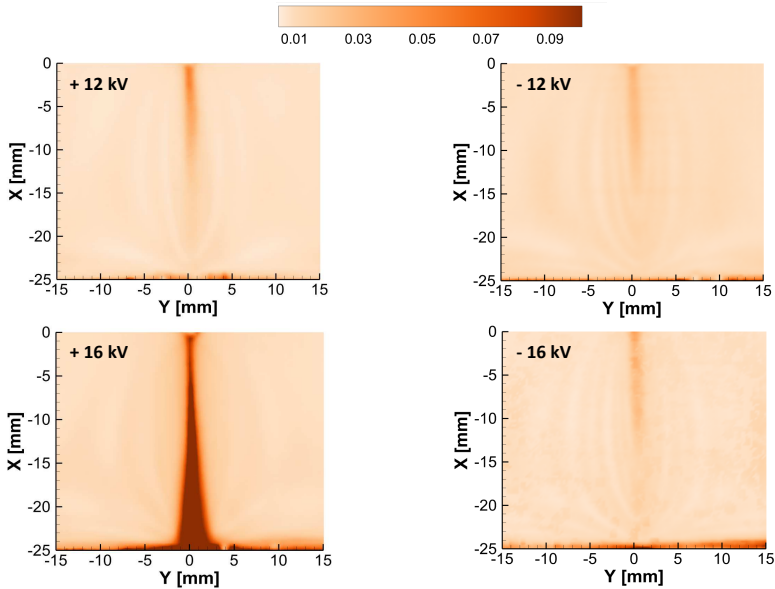


Fig. 7. RMS velocity fields for positive (left) and negative (right) discharges, at 12 kV and 16 kV.

To deepen this phenomenon, we extracted the streamwise velocity from instantaneous velocity fields midway between the needle and the plate and we computed the velocity power spectra density (PSD). The results showed us that the PSD of the velocity is composed of a strong fundamental peak (around 3.3 kHz for $V = 16$ kV, see Fig. 8a) as well as several harmonics, whereas no frequency peak is visible in the case of a glow regime (not shown here). By computing the PSD of the corresponding discharge current (presented in Fig. 2), we can highlight that the frequency of the current peaks, related to the streamer propagation, is totally matching the one of the ionic wind pulses (Fig. 8b). This means that the EHD flow dynamics is fully affected by the streamer occurrence.

How to explain this observation? Indeed, one can assume that although an increase in the time-averaged velocity is observed when streamers occur, there is no ionic wind during the streamer propagation because the streamer correspond to an ionization wave, without ion displacement. The streamer velocity is typically equal to about 1 mm/ns, corresponding to a mean streamer duration of about 25 ns for an electrode gap equal to 25 mm. In our case, as illustrated by Figure 8c that presents a zoomed view of one single discharge current pulse versus time, one can observe that its duration (≈ 600 ns) is largely higher than the one of a typical single streamer. That means that each primary streamer is followed by several secondary streamers, as it has been explained by Marode in [3]. Then, after these secondary streamers, a significant positive space charge remains in the inter-electrode gap and positive ions drift under the effect of the electric field, resulting in a high EHD force.

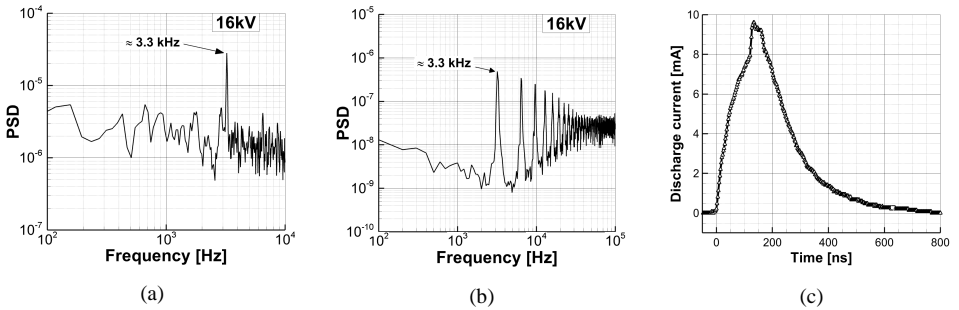


Fig. 8. Power spectra density (PSD) of the ionic wind velocity at $x = 12.5$ mm and $y = 0$ (a), PSD of the discharge current (b) and zoom of one current peak (c), this plot being a time average of 100 current peaks.

IV. CONCLUSION

In this paper, we studied the ionic wind produced by positive and negative corona discharges and we tried to link its characteristics with the electrical and optical properties of the discharge. We highlighted that the time-averaged velocity of the ionic wind produced by both negative and positive coronas is fully different. For the negative corona, the velocity is maximum inside a region close to the point, this region growing and spreading progressively toward the plate when the high voltage is increased. For the positive corona discharge, up to +12 kV, the region of maximum velocity is also located near the point. From +14 kV, when the breakdown streamer regime appears, the mean velocity becomes constant along the x axis, meaning that there is still a weak EHD force in the electrode gap to counter the viscous forces.

Moreover, the temporal analysis of the ionic wind allows us to show that a negative corona discharge produces a steady ionic wind with weak velocity fluctuations because its current is continuous. On the contrary, the positive discharge induces a faster ionic wind, showing that it is more efficient than the negative discharge in ionic wind production, more especially when the breakdown streamer regime appears. However, the presence of streamers results in an unsteady flow with strong velocity fluctuations at the streamer frequency.

ACKNOWLEDGMENTS

This work has been funded by the French Government program INVESTISSEMENT D'AVENIR (LABEX INTERACTIFS, reference ANR-11-LABX-0017-01).

REFERENCES

- [1] Townsend, J. S. & Edmunds, P. J. (1914). "The discharge of electricity from cylinders and points. *Philos. Mag. Ser. 6* 27, 789–801.
- [2] Nouri, H., Zouzou, N., Moreau, E., Dascalescu, L. & Zebboudj, Y. (2012). "Effect of relative humidity on current–voltage characteristics of an electrostatic precipitator". *J. Electrostat.* 70, 20–24.
- [3] Marode, E. (1975). "The mechanism of spark breakdown in air at atmospheric pressure between a positive point and a plane I. Experimental: Nature of the streamer track", *J. Appl. Phys.* 46, 2005–2015.